Pakistan Veterinary Journal

ISSN: 0253-8318 (PRINT), 2074-7764 (ONLINE)
DOI: 10.29261/pakvetj/2026.194

RESEARCH ARTICLE

The Association of Serum Ferritin Levels with Endometriosis: A Machine Learning-Based analysis of NHANES Data, adjusted for Pet Exposure

Sensen Shi[1#], Zelong Li[1#], Xinyue Wu [2], Ziyi Xu [2] and Junfeng Li[1*]

[1]Department of Gynecologic Oncology, Fujian Maternity and Child Health Hospital College of Clinical Medicine for Obstetrics & Gynecology and Pediatrics, Fujian Medical University, Fuzhou, Fujian Province 350001, P. R. China.
[2]College of Veterinary Medicine, Nanjing Agricultural University, Nanjing, 210095, China
# These authors contributed equally to this work.
*Corresponding author: lijunfeng@fjsfy.com

ARTICLE HISTORY (26-869)

Received: July 13, 2026
Revised: August 13, 2026
Accepted: August 18, 2026
Published online: August 26, 2026

Key words:
Endometriosis
Machine Learning
Random Forest Model
Serum Ferritin

A B S T R A C T

Endometriosis has been linked to disturbances in iron metabolism; however, the association between circulating ferritin concentrations and prevalent endometriosis remains uncertain. We aimed to examine the association between serum ferritin concentrations and self-reported physician-diagnosed endometriosis and to evaluate machine-learning models for classifying endometriosis status. This cross-sectional study included 4,448 women aged ≥18 years from the 1999–2006 National Health and Nutrition Examination Survey, of whom 316 reported a physician diagnosis of endometriosis. Survey-weighted multivariable logistic regression and restricted cubic spline analyses were used to evaluate the association between serum ferritin concentrations and the prevalence odds of endometriosis. Following feature selection, decision tree, naïve Bayes, random forest, and support vector machine models were developed using a 70:30 training-test split and evaluated using 10-fold cross-validation. Model discrimination was assessed using the area under the receiver operating characteristic curve, and SHAP analysis was used to examine feature contributions. Serum ferritin concentrations were higher among participants with self-reported physician-diagnosed endometriosis than among those without endometriosis. After multivariable adjustment, participants in the highest ferritin quartile had significantly higher odds of reporting physician-diagnosed endometriosis than those in the lowest quartile (adjusted OR, 2.19; 95% CI, 1.28–3.74). Restricted cubic spline analysis suggested a nonlinear association between serum ferritin and endometriosis (P for nonlinearity = 0.001). Among the four machine-learning models, the random forest model showed the highest discrimination, with an AUROC of 0.862. Higher serum ferritin concentrations were positively associated with self-reported physician-diagnosed endometriosis. The random forest model showed promising internal discrimination; however, prospective studies and external validation are required before the model can be considered for clinical application.

To Cite This Article: Shi S, Li Z, Wu X, Xu Z and Li J, 2026. the association of serum ferritin levels with endometriosis: a machine learning-based analysis of NHANES data, adjusted for pet exposure. Pak Vet J, 46(8): 2043-2054. http://dx.doi.org/10.29261/pakvetj/2026.194

INTRODUCTION

Endometriosis is characterized by the atypical growth of endometrial tissue in locations beyond the confines of the uterine cavity, often affecting the ovaries, pelvic region, and additional remote organs. (Girling, 2024). This condition affects roughly 10% of women in their reproductive years and is the primary contributor to chronic pelvic pain and infertility (Paiva *et al*., 2015; Shafrir *et al*., 2018; Zondervan *et al*., 2020; Gete *et al*., 2024; Harder *et al*., 2024) and carries a potential risk of malignant disease (Mishra *et al*., 2020; Shigetomi *et al*., 2022).

Recent evidence suggests that external factors, including viral infections such as SARS-CoV-2, may also influence female reproductive outcomes and laboratory

parameters related to fertility (Hu *et al*., 2024). Diagnosis is often delayed by 7-10 years due to the non-specific symptoms and limitations in imaging sensitivity and specificity (Zhang *et al*., 2023; Shaukat *et al*., 2025). The current rASRM staging system, which relies on laparoscopy (Zondervan *et al*., 2020; De Corte *et al*., 2025), lacks early identification markers for high-risk cases, highlighting the critical necessity for non-invasive, readily accessible, and easily interpretable screening modalities. Endometriosis is now acknowledged not only as an estrogen-dependent chronic inflammatory condition but also as a disorder linked to systemic irregularities in iron metabolism. Mounting evidence suggests that disturbances in iron metabolism may serve as systemic drivers influencing the progression of the disease (Shigetomi *et al*., 2022; Liu *et al*., 2023; Kang *et al*., 2024; Huang *et al*., 2025).

Iron is an essential element for all living organisms, and intracellular iron homeostasis pertains to the equilibrium among iron uptake, iron efflux, utilization, and storage. An overload of iron can increase the risk of tissue injury and development of cancer (Duan *et al*., 2024; Liu *et al*., 2024). Ferritin is a cellular protein essential for the export of cellular iron to sustain this equilibrium. A total of approximately 4500 iron atoms can be bound by this protein, which consists of two subunits: ferritin light chain and ferritin heavy chain 1. The ferritin complex effectively sequesters trivalent iron (Fe^{3+}) that is not successfully reduced to ferrous iron (Fe^{2+}) by divalent metal transporter 1 (DMT1) to mitigate the risk of oxidative damage caused by the Fenton reaction (Hassannia *et al*., 2019; Liu *et al*., 2023). The Fenton reaction is a biochemical process that generates reactive oxygen species (ROS). It produces hydroxyl radicals within cellular environments. This reaction occurs when ferrous iron (Fe^{2+}) interacts with hydrogen peroxide (H_2O_2), resulting in the production of hydroxyl radicals (OH). Disruption of iron homeostasis causes intracellular or extracellular accumulation of free iron. Excess iron triggers the Fenton reaction, leading to oxidative damage to DNA, lipid, and cell membrane (Toyokuni, 2002; Liu *et al*., 2024). It also affects parenchymal organs like the liver, pancreas, kidneys, and heart (Liu *et al*., 2022). Ferritin is subject to phagocytosis, a process that is modulated by nuclear receptor coactivator 4 ($NCOA_4$), which aids in the controlled release of stored Fe^{2+} as required. Nevertheless, an overabundance of Fe^{2+} released from serum ferritin has the potential to initiate the Fenton reaction, thereby possibly resulting in ferroptosis (Santana-Codina *et al*., 2022; Liu *et al*., 2023). Above process promote inflammation (Li *et al*., 2022; Zhang *et al*., 2024) and oxidative stress (Hayashi *et al*., 2020; Zhang *et al*., 2022), which both of which subsequently play a significant role in the advancement of endometriosis (Ngô *et al*., 2009; Zhang *et al*., 2024a).

Although iron overload and ferroptosis have been extensively researched (Kobayashi *et al*., 2024; Luo *et al*., 2024), the role of serum ferritin, a iron storage protein, in endometriosis remains insufficiently investigated. Previous studies indicated elevated ferritin levels in endometriosis tissue, highlighting its role as a key biomarker in disease pathogenesis (Luque-Ramírez *et al*., 2007; Liu *et al*., 2022; Xu *et al*., 2023). The prevalence of endometriosis and serum ferritin concentrations are positively correlated in the NHANES database (Xu *et al*., 2023).

A previous cross-sectional analysis of NHANES data reported positive nonlinear associations between serum ferritin concentrations, transferrin saturation, and prevalent endometriosis. However, the relative contribution of serum ferritin within multivariable machine-learning classification models, alongside sociodemographic, reproductive, and other iron-related variables, remains incompletely characterized. To address this gap, we examined the association between serum ferritin concentrations and the prevalence odds of self-reported physician-diagnosed endometriosis among women participating in NHANES 1999–2006 (Brulport *et al*., 2024).

We additionally developed and internally evaluated machine-learning models for classifying self-reported endometriosis status and applied SHAP analysis to assess the relative contribution of serum ferritin and other model features. Given the cross-sectional design, these analyses were intended to characterize associations with prevalent endometriosis and classification performance rather than to predict future disease onset (Avery *et al*., 2024).

MATERIALS AND METHODS

Data sources and test populations: The National Health and Nutrition Examination Survey (NHANES) is a biennial initiative carried out by the Centers for Disease Control and Prevention (CDC). The dataset utilized in this research was obtained from the National Center for Health Statistics (NCHS) and includes information from four NHANES cycles spanning 1999 to 2006. From the initial cohort of 41,474 individuals, we excluded male participants (n=20,264) and individuals under 18 (n=8,406). We also excluded cases with missing endometriosis data from interviews (n=6,301) and those with incomplete data on serum iron, serum ferritin, total iron-binding capacity, transferrin saturation, and other key covariates (n=1,109). The outcome variable was endometriosis diagnosis, based on participants' self-reported physician diagnoses. Participants who met these criteria were classified as the Endometriosis group. All other participants were included in the non-Endometriosis group. Only records with complete Endometriosis information were retained, resulting in a final analytic sample of 4,448 women—316 with Endometriosis and 4,132 without. In Figure 1, the selection methodology is illustrated.

The study protocol was approved by the NCHS Ethics Review Committee, and all participants provided written informed consent. The NHANES data are de-identified and publicly available, so this study is exempt from additional IRB review.

Exposure and outcome variables: Serum Iron: Fasting venous blood samples were collected from participants. Serum iron concentration (μg/dl) is measured directly in serum using a colorimetric method based on the ferrozine reaction (NHANES Laboratory Data Files: LAB06 for 1999-2000, L40FE for 2001-2002, L40FE for 2003-2004, FETIB for 2005-2006). This approach measures the amount of iron bound to transferrin in the bloodstream.

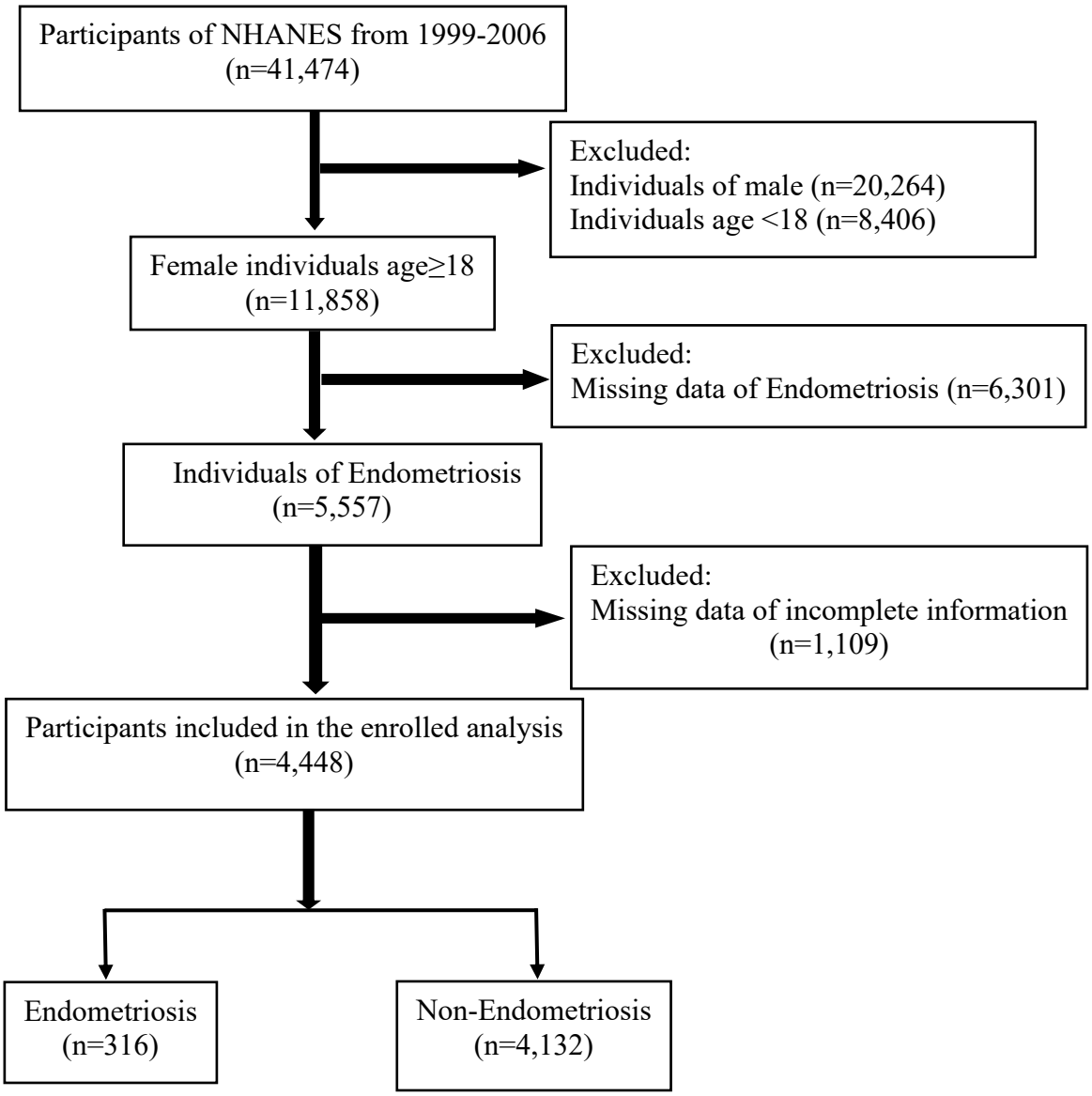

Fig. 1: Flow-chart of the NHANES study participants.

Serum Ferritin: Serum ferritin concentrations were reported in ng/mL. In the 1999–2002 cycles, ferritin was measured using the Bio-Rad QuantImune Ferritin immunoradiometric assay (IRMA). During the 2003–2004 cycle, samples collected in 2003 were initially measured using the Bio-Rad assay, whereas samples collected in 2004 were measured using an immunoturbidimetric assay on the Roche/Hitachi 912 analyzer. Ferritin measurements in 2005–2006 were also obtained using the Roche/Hitachi immunoturbidimetric method. To harmonize measurements across assay methods, ferritin values obtained using the Bio-Rad assay in 1999–2002 were converted to the Roche/Hitachi scale using the piecewise linear regression equations recommended by NHANES: for Bio-Rad ferritin values ≤25ng/mL, adjusted ferritin = 1.2534 × ferritin + 1.4683; for values >25 to ≤65ng/mL, adjusted ferritin = 1.2001×ferritin + 1.4693; and for values >65ng/mL, adjusted ferritin = 1.0791×ferritin + 4.8183. The 2003 ferritin values in the released NHANES 2003–2004 file had already been harmonized to the Roche/Hitachi scale. No additional assay conversion was applied to the 2004–2006 Roche/Hitachi measurements.

Total Iron-Binding Capacity (TIBC): TIBC (μmol/L), reflecting the total amount of iron that transferrin can bind, was measured using a two-step assay. The first step involved saturating transferrin with iron, followed by removing unbound iron. The bound iron was then released and measured using a ferrozine colorimetric assay (NHANES Laboratory Data Files: LAB06 for 1999-2000, L40FE for 2001-2002, L40FE for 2003-2004, FETIB for 2005-2006).

Transferrin Saturation: Transferrin saturation (TSAT, %) was calculated by dividing serum iron by TIBC and then multiplying by 100 (TSAT = (serum Iron/TIBC)×100%).

Extensive quality assurance details are accessible on the NHANES website. Before each survey session, the instruments are carefully calibrated and rigorously tested for quality control.

The diagnosis of endometriosis was established based on responses to questions from the Reproductive Health (RHQ) (variable name prefix RHQ360): (1) Has a doctor or other health professional ever told you that you had endometriosis? Participants were then categorized as having endometriosis or not, based on their Yes or No answers to a series of questions.

Covariates: To minimize confounding, the analysis accounted for a range of sociodemographic and clinical variables. Covariates included race, educational level, smoking status, alcohol consumption status, poverty-to-income ratio (PIR), body mass index (BMI), history of oral contraceptive use (ever used birth control pills), pregnancy history (ever been pregnant), and marital status. Age was categorized into three brackets: 18–45, 46–60 and >60 years, while BMI was categorized as underweight (<18.5kg/m²), normal weight (18.5–24.9kg/m²) and overweight or obese (≥25.0kg/m²). PIR was stratified as <1.0, 1–3 and >3.0 to reflect economic status. Age, serum iron, and total iron-binding capacity were also treated as continuous covariates in the regression models. Variable definitions and measurement protocols, detailed in the NHANES documentation, were followed in this study.

Household pet exposure variables were derived from the HOQ questionnaire, including indicators for dogs, cats, and small furry animals in the household currently (HOQ260A–C) and within the past 12 months (HOQ280A–C). All datasets were merged at the participant level using the unique identifier SEQN across survey cycles. For analysis, a composite binary exposure variable (ANY_PET) was created, defined as the presence of any household pet based on positive responses across HOQ260A–C or HOQ280A–C.

Statistical analysis: Due to NHANES's complex multistage sampling strategy, all statistical analyses incorporated sampling weights to ensure population-level representativeness and reduce potential estimation bias. Participants were classified into two groups: those with endometriosis and those without endometriosis. Continuous variables are summarized using the median and interquartile range (IQR), whereas categorical variables are expressed in terms of counts and percentages. For group comparisons, the Wilcoxon rank-sum test (also known as the Mann-Whitney U test) and Pearson's chi-square test were utilized. Unweighted counts and descriptive summaries were reported to characterize the actual analytic sample and provide transparency regarding the number and distribution of observed participants. Survey-weighted estimates were considered the primary results for population-level inference because they account for the complex NHANES sampling design.

To assess the association between serum ferritin concentrations and the odds of self-reported physician-diagnosed endometriosis, we fitted three survey-weighted logistic regression models. In these models, endometriosis was the dependent variable, while serum ferritin and various covariates served as independent variables. Three logistic models were included: Model 1 (unadjusted), Model 2 (adjusted for age and race) and Model 3 (fully adjusted for sociodemographic and clinical factors including educational attainment, PIR, alcohol use, smoking, BMI, use of birth control pills, pregnancy status, marital status, serum iron, and TIBC. Serum ferritin quartiles were analyzed to assess dose-response trends (P for trend). Subgroup analyses using Model 3 were performed to evaluate consistency across different strata and test for interactions. To explore potential nonlinear associations, we applied RCS models for serum ferritin across all three models. Furthermore, RCS regression was performed for age and fertility strata to assess these nonlinear patterns among diverse populations.

Machine learning methods are more suitable for analyzing large-scale data than traditional statistical methods. These approaches facilitate the automatic enhancement of model efficacy by employing strategies such as parameter tuning and cross-validation (Li *et al*., 2023; Wang *et al*, 2024; Guo *et al*., 2025). Machine learning technology demonstrates high performance across various domains (Guo *et al*., 2024; Guo *et al*., 2025). In the present investigation, we constructed a predictive model for endometriosis using carefully chosen variables. The Minimum Absolute Shrinkage and Selection Operator (Lasso) was utilized to pinpoint and choose essential features that significantly contribute to the predictive model. Conversely, the Boruta algorithm serves as a powerful feature selection method grounded in the principles of random forest analysis. It evaluates the relevance of the initial features by juxtaposing their importance scores with those of the shadow features (Tan *et al*., 2025). We selected the variables related to the prediction through Lasso regression and Boruta algorithm. Due to the imbalance of the samples, we first screened the relevant variables and then adjusted the data using the SMOTE over-sampling method. Next, we standardized the features. Afterwards. The dataset was randomly partitioned into two distinct subsets. One subset, comprising 70% of the data, was designated as the training set to construct the predictive models. The remaining 30% was reserved as the test set to evaluate model performance (Zuo *et al*., 2025). Four machine learning algorithms—Decision Tree, Naive Bayes, Random Forest, and Support Vector Machine (SVM)—were developed using the training dataset to build and evaluate prediction models estimating the likelihood of endometriosis occurrence (Paiva *et al*., 2015). Internal validation was executed through 10-fold cross-validation. Confusion matrices were utilized to evaluate the models. Additionally, SHAP analysis was implemented to enhance the interpretability of the models by identifying the significance of each feature and elucidating the rationale behind the decisions made.

All statistical analyses were performed using the DecisionLinnc Data Science Platform (version 1.1.6.7; RRID: SCR_026971), which integrates R and Python computational environments. Survey-weighted descriptive analyses and logistic regression, restricted cubic spline modeling, and LASSO regression were conducted using the corresponding R-based modules. Boruta feature selection and synthetic minority over-sampling technique (SMOTE) were implemented using the corresponding modules available within DecisionLinnc. Decision tree, Gaussian naïve Bayes, random forest and support vector machine classifiers were implemented in Python using

scikit-learn. Ten-fold cross-validation and model-performance evaluation were also conducted using scikit-learn. SHAP-based model interpretation was performed using the R-based SHAP module available within DecisionLinnc. All statistical tests were two-sided, and a P value <0.05 was considered statistically significant.

RESULTS

Baseline demographic and clinical characteristics of participants: The analysis included 4448 women aged 18 or older who met the eligibility criteria from the 1999–2006 NHANES dataset (Fig. 1). Of the participants, 316 had endometriosis. Serum ferritin levels were 77.97ng/mL versus 55.67ng/mL in the weighted analysis (P<0.001). Furthermore, the endometriosis group showed a greater prevalence of non-Hispanic white individuals (P<0.001), higher education levels (predominantly college and above) and more smokers. Moreover, a significantly higher of women with endometriosis reported the use of oral contraceptives (P<0.001), in agreement with known risk profiles**.**

Table 1 presents unweighted sample summaries alongside survey-weighted population estimates. Unweighted values are provided to describe the observed analytic sample, whereas weighted estimates constitute the primary results for population-level comparisons. In the weighted analysis, participants with self-reported physician-diagnosed endometriosis had higher serum ferritin concentrations than those without endometriosis (77.97 vs 55.67ng/mL; P<0.001) and higher transferrin saturation (24.21% vs 22.66%; P=0.010).

Several descriptive estimates, particularly the distributions of race/ethnicity, educational attainment, and poverty-to-income ratio, differed between the unweighted sample summaries and the survey-weighted population estimates. These differences reflect the unequal probabilities of selection and the complex sampling design of NHANES and support the use of survey-weighted estimates as the primary basis for population-level inference.

The prevalence of endometriosis was 6.6% among individuals without pets (319/4838) and 8.5% among those with pets (61/719). Although the proportion was slightly higher in the pet-exposed group, this difference did not reach statistical significance (P=0.073), indicating no evidence of an association between pet ownership and endometriosis in this unadjusted analysis.

Table 1: Basic characteristics of the endometriosis and the non-endometriosis groups enrolled in the NHANES cross-sectional study

Characteristic	Total n=4448	weighted N = 52,959,570	data Non-Endometriosis n=4132	Non-Endometriosis (weighted) N = 47,945,062	Endometriosis n=316	Endometriosis (weighted) N = 5,014,508	p
Serum_ferritin(ng/ml)	53.16 (71.12)	57.78 (66.30)	51.087±60.077	55.67 (57.62)	80.23 (152.57)	77.97 (119.47)	<0.001
Serum_iron(ug/dL)	80.12 (39.20)	82.69 (38.73)	79.901±39.435	82.42 (38.95)	83 (35.88)	85.28 (36.52)	0.084
Tibc (ug/dL)	388.21 (74.89)	374.43 (63.90)	389.518±74.965	375.57 (64.03)	371.17 (71.87)	363.59 (61.68)	0.091
Tsat (%)	21.49 (11.24)	22.81 (11.36)	21.358±11.291	22.66 (11.42)	23.16 (10.46)	24.21 (10.69)	0.010
Age (%)							
18-45years	3737 (84.02%)	42,190,189 (79.66%)	3494 (84.56%)	38,411,483 (80.12%)	243 (76.90%)	3,778,706 (75.36%)	0.066
46-60years	711 (15.98%)	10,769,382 (20.34%)	638 (15.44%)	9,533,579 (19.88%)	73 (23.10%)	1,235,802 (24.64%)	
Race (%)							
Mexican American	1063 (23.90%)	4,364,876 (8.24%)	1035 (25.05%)	4,235,340 (8.83%)	28 (8.86%)	129,536 (2.58%)	<0.001
Non Hispanic Black	210 (4.72%)	2,957,735 (5.58%)	203 (4.91%)	2,848,358 (5.94%)	7 (2.22%)	109,377 (2.18%)	
Non Hispanic White	2101 (47.23%)	36,792,107 (69.47%)	1878 (45.45%)	32,512,428 (67.81%)	223 (70.57%)	4,279,679 (85.35%)	
Other Hispanic	881 (19.81%)	6,138,762 (11.59%)	834 (20.18%)	5,802,580 (12.10%)	47 (14.87%)	336,182 (6.70%)	
Other Race	193 (4.34%)	2,706,090 (5.11%)	182 (4.40%)	2,546,356 (5.31%)	11 (3.48%)	159,734 (3.19%)	
Education (%)							
Less than High school graduate	1027 (23.09%)	7,780,175 (14.69%)	994 (24.06%)	7,318,743 (15.26%)	33 (10.44%)	461,432 (9.20%)	<0.001
High school graduate	968 (21.76%)	12,011,807 (22.68%)	886 (21.44%)	10,487,792 (21.87%)	82 (25.95%)	1,524,015 (30.39%)	
College above	2453 (55.15%)	33,167,588 (62.63%)	2252 (54.50%)	30,138,527 (62.86%)	201 (63.61%)	3,029,061 (60.41%)	
Smoking (%)							
No	2770 (62.28%)	30,453,420 (57.50%)	2598 (62.88%)	27,945,437 (58.29%)	172 (54.43%)	2,507,984 (50.01%)	0.018
Yes	1678 (37.72%)	22,506,150 (42.50%)	1534 (37.12%)	19,999,625 (41.71%)	144 (45.57%)	2,506,525 (49.99%)	
Ratio of income to poverty level(%)							
<1	944 (21.22%)	8,375,075 (15.81%)	902 (21.83%)	7,799,082 (16.27%)	42 (13.29%)	575,993 (11.49%)	0.049
1--3	1700 (38.22%)	18,157,647 (34.29%)	1598 (38.67%)	16,633,967 (34.69%)	102 (32.28%)	1,523,680 (30.39%)	
>3	1804 (40.56%)	26,426,849 (49.90%)	1632 (39.50%)	23,512,014 (49.04%)	172 (54.43%)	2,914,835 (58.13%)	
Alcohol (%)							
No	1717 (38.60%)	16,813,076 (31.75%)	1617 (39.13%)	15,398,768 (32.12%)	100 (31.65%)	1,414,308 (28.20%)	0.301
Yes	2731 (61.40%)	36,146,495 (68.25%)	2515 (60.87%)	32,546,295 (67.88%)	216 (68.35%)	3,600,200 (71.80%)	
Bmi (%)							
<18.5	107 (2.41%)	1,688,165 (3.19%)	99 (2.40%)	1,532,621 (3.20%)	8 (2.53%)	155,544 (3.10%)	0.768
18.5-24.9	1425 (32.04%)	19,959,083 (37.69%)	1322 (31.99%)	18,176,355 (37.91%)	103 (32.59%)	1,782,728 (35.55%)	
≥25	2916 (65.56%)	31,312,322 (59.12%)	2711 (65.61%)	28,236,086 (58.89%)	205 (64.87%)	3,076,236 (61.35%)	
Birth_control_pills (%)							
No	1032 (23.20%)	10,029,593 (18.94%)	1002 (24.25%)	9,613,643 (20.05%)	30 (9.49%)	415,950 (8.29%)	<0.001
Yes	3416 (76.80%)	42,929,977 (81.06%)	3130 (75.75%)	38,331,419 (79.95%)	286 (90.51%)	4,598,558 (91.71%)	
Marital_status (%)							
Yes	2903 (65.27%)	34,826,862 (65.76%)	2693 (65.17%)	31,413,718 (65.52%)	210 (66.46%)	3,413,144 (68.07%)	0.439
No	1545 (34.73%)	18,132,708 (34.24%)	1439 (34.83%)	16,531,344 (34.48%)	106 (33.54%)	1,601,364 (31.93%)	
Pregnant (%)							
No	700 (15.74%)	10,876,989 (20.54%)	655 (15.85%)	10,141,777 (21.15%)	45 (14.24%)	735,212 (14.66%)	0.030
Yes	3748 (84.26%)	42,082,581 (79.46%)	3477 (84.15%)	37,803,286 (78.85%)	271 (85.76%)	4,279,296 (85.34%)	
First_menstrual_period_age	28.52 (124.51)	31.88 (136.65)	29.04 (126.43)	32.92 (140.13)	21.75 (95.84)	21.94 (96.76)	0.051

Values are presented as unweighted sample estimates and survey-weighted population estimates. Continuous variables are reported as median (interquartile range), and categorical variables are reported as n (%) for unweighted data and weighted N (%) for survey-weighted data. P values were obtained from survey-weighted comparisons between participants with and without self-reported physician-diagnosed endometriosis. Abbreviations: BMI, body mass index; IQR, interquartile range; PIR, poverty-to-income ratio; TIBC, total iron-binding capacity; TSAT, transferrin saturation.

Association between serum ferritin concentrations and the odds of endometriosis: In a continuous modeling approach, higher serum ferritin concentrations were consistently associated with higher odds of self-reported physician-diagnosed endometriosis. This association was evident in the analysis of three models. Specifically, when adjusting from Model 1 to Model 2 which included age and race, and then to Model 3 which included all covariates, a trend of increased risk in the endometriosis group could be observed as serum ferritin levels rose. The corresponding odds ratios were 1.004 (95% confidence interval, 1.002-1.006, P=0.001), 1.004 (95% confidence interval, 1.002-1.006, P=0.001) and 1.003 (95% confidence interval, 1.0001-1.005, P=0.0016), respectively; these levels indicate a statistically significant association.

Importantly, within the framework of iron homeostasis, only serum ferritin demonstrated a noteworthy independent relationship with endometriosis, regardless of demographic variables and other serum assay results (Table 2).

Table 2: Weighted logistic regression analysis of serum ferritin and TSAT in relation to endometriosis

	Model 1		Model 2		Model 3	
	OR (95%CI)	P-value	OR (95%CI)	P-value	OR (95%CI)	P-value
Serum ferritin	1.004(1.002-1.006)	<0.001	1.004(1.002-1.006)	<0.001	1.003(1.0001-1.005)	0.0016
	Model 1		Model 2		Model 3	
	OR (95%CI)	P-value	OR (95%CI)	P-value	OR (95%CI)	P-value
TSAT	1.01(1.00-1.02)	0.035	1.008(0.997-1.019)	0.155	1.02(0.96-1.08)	0.514

Weighted logistic regression analysis shows that demographic and clinical variables affect the relationship between TSAT and endometriosis risk. As a result, TSAT is excluded from risk assessments in subsequent trend analyses.

To further assess dose–response trends, serum ferritin was categorized into quartiles: Q1 (9.739±4.531), Q2 (25.766±4.867), Q3 (48.235±8.883) and Q4 (130.481±107.551) (see Table 3). In statistical Models 1 and 2, Participants in the higher serum ferritin quartiles, particularly Q4, had higher odds of self-reported physician-diagnosed endometriosis. While the *p*-values for Q2 and Q3 did not reach statistical significance in Model 3, Q4 exhibited a statistically significant, indicating a notable increasing trend in odds ratio values with increasing serum ferritin levels. This trend requires confirmation in larger or prospective studies. Across Models 1 to 3, which included various covariates such as demographic and clinical factors, a significant trend in quartile differences was observed (P<0.001 for trend). Endometriosis is associated with elevated serum ferritin levels, regardless of covariates.

The trend analysis showed significant differences among quartiles (P<0.001 for trend) after adjusting for demographic and clinical covariates. These findings indicate that women with higher serum ferritin concentrations had higher odds of self-reported physician-diagnosed endometriosis, irrespective of their demographic or clinical profiles.

Subgroup analysis exploration: Subgroup analyses were performed to investigate the relationships among different populations and clinical subcategories, which were stratified by age, race, smoking status, education, BMI, and alcohol consumption (Fig. 2).

The association between serum ferritin concentrations and the odds of self-reported physician-diagnosed endometriosis varied across some subgroups; however, statistically significant interaction was observed only for age and alcohol consumption. The results showed that elevated serum ferritin concentrations were associated with endometriosis in women aged 18 to 45 years, with an odds ratio of 1.58 (95% confidence interval, 1.25-2.01, P=0.001). Furthermore, elevated serum ferritin levels were notably linked to endometriosis in non-Hispanic black women, non-Hispanic white women, smokers, and alcohol consumers, with ORs of 1.71 (95% CI, 1.29-2.27), 1.37 (95% CI, 1.1-1.7), 1.44 (95% CI, 1.14-1.83) and 1.62 (95% CI, 1.27-2.05), respectively. The corresponding P-values were P=0.001, 0.007, 0.004, and <0.001 and these analyses were adjusted for covariates including poverty index, marital status, fertility status, and the utilization of oral contraceptives.

Table 3: Weighted trend test analysis of serum ferritin

		Model1		Model2		Model3	
		OR(95%CI)	p-value	OR(95%CI)	p-value	OR(95%CI)	p-value
Serum ferritin		1.004(1.002-1.006)	**<0.001**	1.004(1.002-1.006)	**<0.001**	1.003(1.0001-1.005)	**0.0016**
Serum ferritin(quartile)							
Q1	9.739±4.531	reference		reference		reference	
Q2	25.766±4.867	1.44(0.88-2.35)	0.14	1.33(0.81-2.18)	0.25	1.28(0.76-1.30)	2.169
Q3	48.235±8.883	1.70(1.02-2.81)	**0.04**	1.56(0.94-2.58)	0.08	1.48(0.86-2.54)	0.149
Q4	130.481±107.551	2.70(1.66-4.39)	**<0.001**	2.49(1.52-4.08)	**0.005**	2.19(1.28-3.74)	**0.005**
p for trend			**<0.001**		**<0.001**		**<0.001**

Model 1: no covariates were adjusted. Model 2: adjusted for age, race. Model 3: adjusted for age, race, Education attainment, PIR, alcohol, smoking, BMI, taken birth control pills, pregnant status, marital status, serum iron and TSAT.

.

Tests for interaction indicated that the association between serum ferritin concentrations and self-reported physician-diagnosed endometriosis differed significantly by age (P for interaction=0.006) and alcohol consumption (P for interaction=0.015). No statistically significant interaction was observed for race/ethnicity (P for interaction=0.731), educational attainment (P for interaction=0.589), smoking status (P for interaction=0.409), or BMI category (P for interaction=0.266).

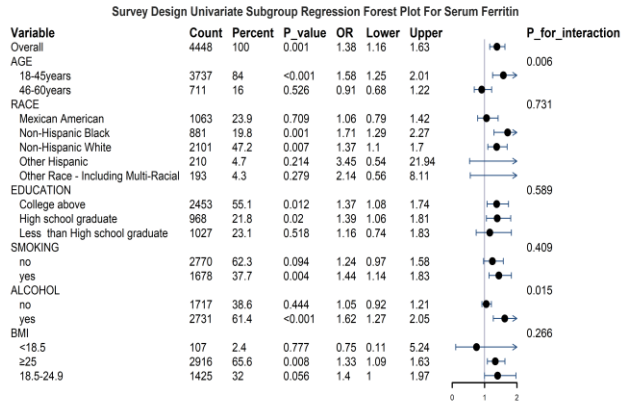

Fig. 2: Survey-weighted multivariable subgroup analyses of the association between serum ferritin concentrations and self-reported physician-diagnosed endometriosis. Models were adjusted for the covariates included in Model 3, excluding the corresponding stratification variable. ORs and 95% CIs are presented for each stratum, together with P values for interaction.

Nonlinear association between serum ferritin concentrations and the odds of endometriosis: In Model 3, we examined the association between serum ferritin levels and the probability of developing endometriosis through RSC analysis. Furthermore, we segmented this relationship based on pertinent clinical risk factors for endometriosis (age and fertility status) to explore potential nonlinear relationships between serum ferritin and endometriosis (Fig. 3).

Overall, the findings indicate a nonlinear dose-response relationship between serum ferritin concentrations and endometriosis risk (P for nonlinear = 0.001). Particularly, when serum ferritin levels surpass a specific threshold (about 30ng/mL), the odds ratio for endometriosis increases as serum ferritin levels rise. Stratified analysis demonstrated that age and fertility status act as effect modifiers. Specifically, the association was notably pronounced in the 46-60 age group (overall P<0.001) and among women who have given birth (overall P<0.001). In contrast, no meaningful association was identified in nulliparous women (P=0.436). These outcomes suggest critical thresholds and population diversity in the impact of iron storage levels.

Machine learning: The current research data exhibit limited positive events and data imbalances. To address this, we employ the SMOTE oversampling method to balance the data for subsequent machine learning. Subsequently, we applied Lasso regression and Boruta test to identify relevant variables (Fig. 4).

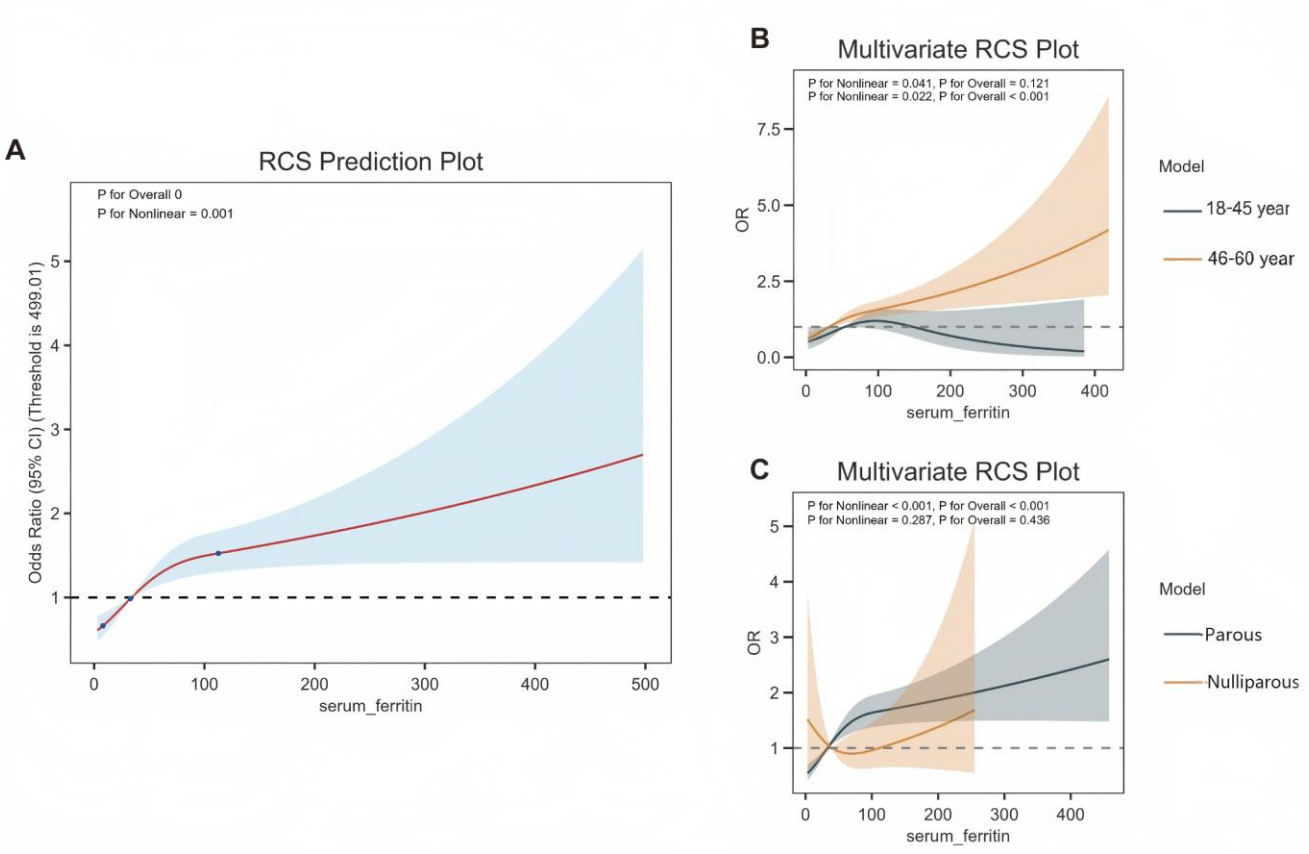

Fig. 3: (A) Dose-response relationship between serum ferritin and endometriosis, adjusted for Model 3. This model has been adjusted for age, race, educational attainment, PIR, alcohol consumption, smoking habits, BMI, use of birth control pills, pregnancy status, marital status, serum iron, and TSAT. (B) The RCS curves stratified by age. (C) The RCS curves stratified by fertility.

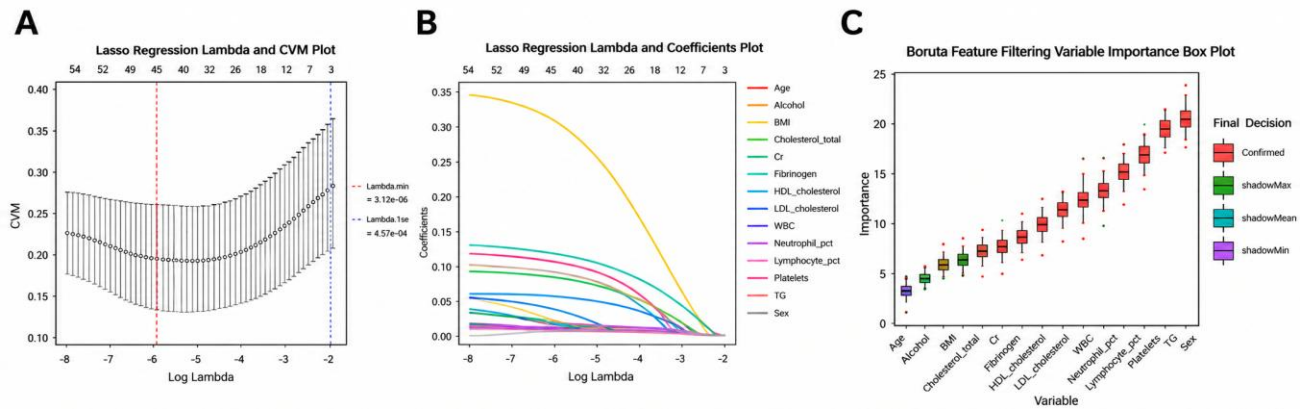

Fig. 4: Lasso regression and Boruta algorithm were utilized for variable selection. (A) Cross-Validation Error (CVM) for various log lambda values is presented. The orange dashed line indicates the point of minimal error (log λ_min), while the blue dashed line signifies the standard error threshold as determined by the model (log λ_1se). (B) Screening Variables Using Lasso Regression Method. The trajectory of each variable's coefficient changes as the log(lambda) value is adjusted, illustrating how variables respond to different levels of regularization. (C) Boruta analysis identified 11 significant variables associated with endometriosis, with serum ferritin ranking as the third most important. The other variables included age, race, PIR, education, alcohol consumption, fertility, BMI, serum iron, transferrin saturation, and total iron-binding capacity.

Based on our analysis, we combined the screening results and identified seven key variables with serum ferritin as the focal point: age, race, serum ferritin, PIR, education level, alcohol consumption and fertility.

Following the application of SMOTE undersampling to achieve data balance on the basis of seven selected variables, four distinct machine learning techniques were employed on the training subset. The result showed that the RF model yielded an AUC of 0.862, higher than Decision Tree (0.833), Naive Bayes (0.663) and SVM (0.727) (Fig. 5). The confusion matrix demonstrated that the RF model achieved superior precision and F1-score, indicating high prediction accuracy.

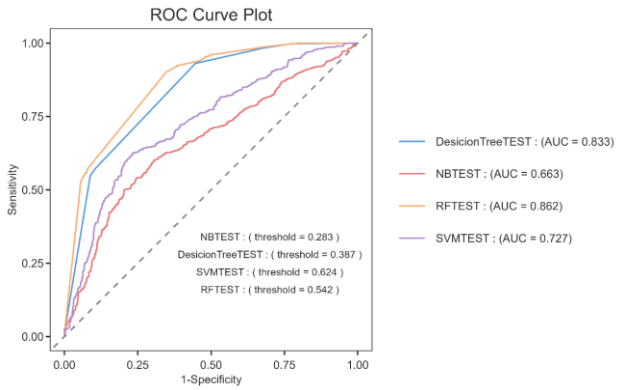

Fig. 5: The effectiveness of four machine learning algorithms was evaluated using the area under the receiver operating characteristic curve.

Table 4: Each model was evaluated using a confusion matrix of accuracy, AUC, precision, recall and F1 score.

Model	Accuracy	Recall	F1-Score	AUROC	Presicion	Specificity
RFTEST	0.790	0.918	0.832	0.862	0.763	0.621
SVMTEST	0.659	0.684	0.695	0.727	0.708	0.626
DesicionTreeTEST	0.769	0.930	0.821	0.833	0.734	0.553
NBTEST	0.627	0.517	0.612	0.663	0.750	0.772

We conducted a more in-depth analysis of variable significance and model performance, focusing on the optimal results produced by the random forest method. This evaluation was carried out by employing SHAP analysis to provide insights into the interpretation of the model (Fig. 6 and Table 4).

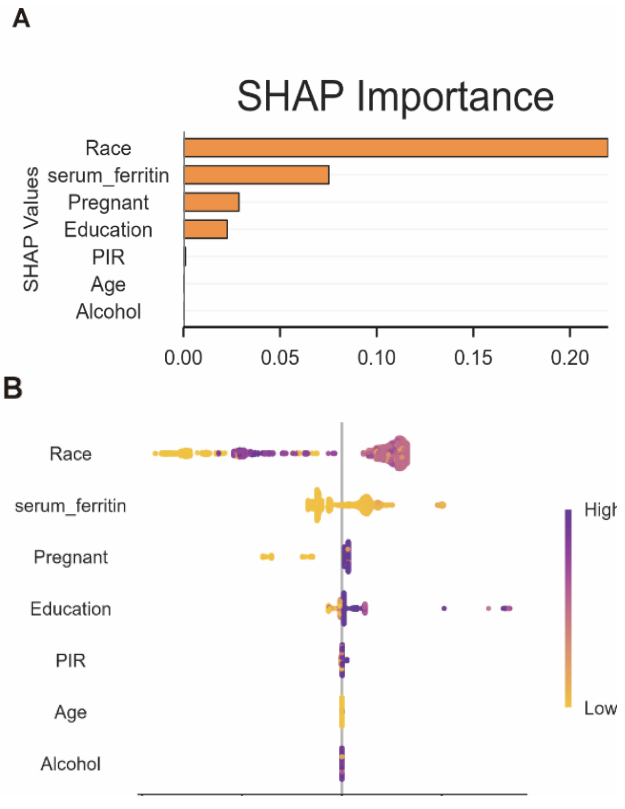

Fig. 6: Explainability analysis of random forest model. (A) Assessment of the significance of features within the model. (B) SHAP tree representation illustrates the attributes of the model.

Fig. 6 shows the SHAP plot, where colors represent the sign of the original eigenvalues—purple for positive and yellow for negative values—and SHAP values indicate the effect of each feature on the outcome, with positive values denoting beneficial effects and negative values denoting adverse effects. Fig. 6A ranks the results by the mean absolute SHAP values to show feature influence. The SHAP summary chart for endometriosis patients identifies race, serum ferritin, pregnancy, and education as the most influential features. Fig. 6B shows that race and serum ferritin are pivotal variables influencing endometriosis and elevated serum ferritin significantly increases the risk.

To evaluate the model's stability, we implemented a 10-fold cross-validation technique. This approach involves dividing the dataset into ten distinct subsets, wherein the model is trained using nine of these subsets while its performance is evaluated on the single remaining subset. This iterative process provides a reliable evaluation of the model's ability to generalize (Zhang *et al*., 2024). The results showed that the random forest method attained a average accuracy of 79.7%, an AUC of 0.8626, and an F1 score of 0.84 (Fig. 7).

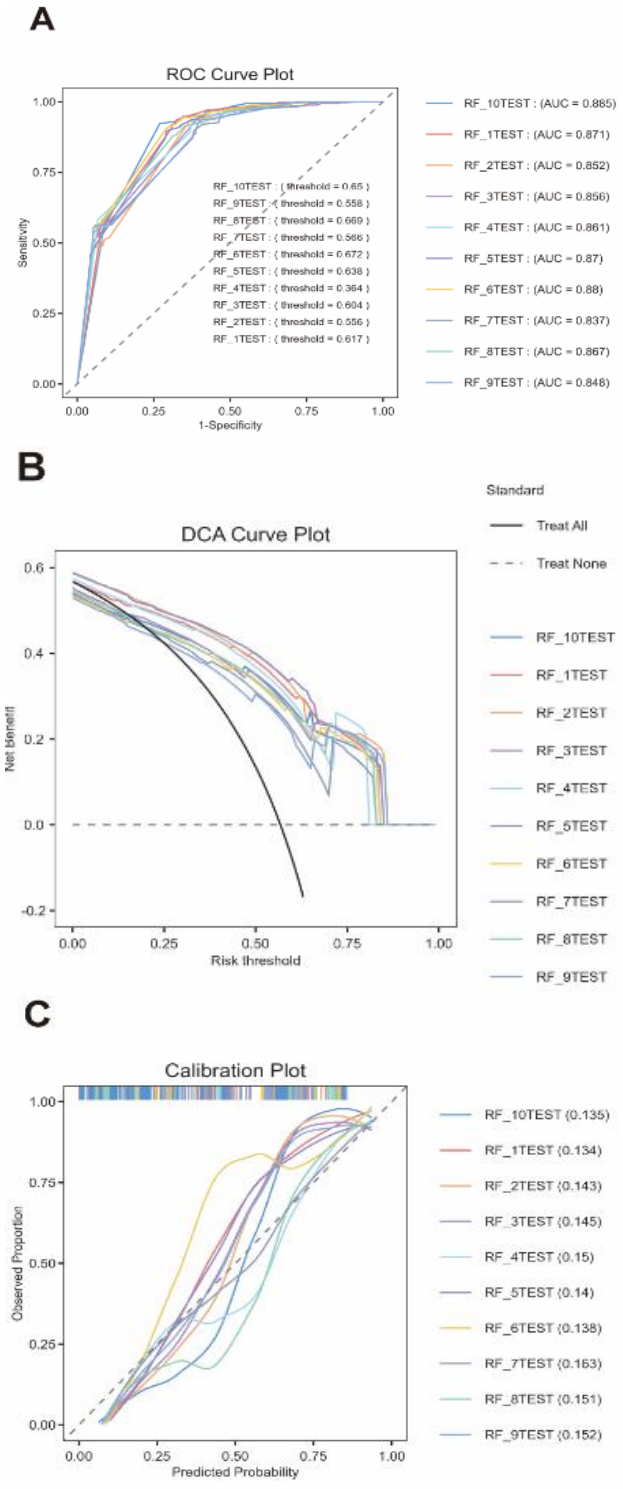

Fig. 7: Model evaluation of random forest method with 10-fold cross validation. (A) ROC curve after cross validation. (B) DCA decision curve after cross validation. (C) Calibration curve after cross validation.

The findings indicate that the random forest method using serum ferritin achieves enhanced predictive performance. Further validation through numerous prospective studies and external verifications is essential to elucidate its efficacy.

DISCUSSION

In this cross-sectional analysis of nationally representative NHANES data, higher serum ferritin concentrations were associated with greater odds of self-reported physician-diagnosed endometriosis after adjustment for relevant sociodemographic, reproductive, and iron-related covariates (Dore and Lagace, 1985; Chin, 1994). Participants in the highest serum ferritin quartile had approximately twice the odds of reporting endometriosis compared with those in the lowest quartile, and restricted cubic spline analysis suggested a nonlinear association. Among the four machine-learning classifiers, the random forest model showed the highest internal discrimination, with an AUROC of 0.862. However, because serum ferritin and endometriosis status were assessed within a cross-sectional framework, the temporal sequence between exposure and outcome cannot be established, and the findings do not demonstrate that elevated serum ferritin causes or precedes endometriosis.

Endometriosis is a persistent inflammatory condition dependent on estrogen and associated with various factors including sex hormones, immune response, inflammatory processes, and genetic predispositions (Duan *et al*., 2024; Yao *et al*., 2026). Recent investigations have indicated a correlation between the accumulation of excess iron and the phenomenon of ferroptosis with the onset and progression of endometriosis. Increased concentrations of iron have been detected in the peritoneal fluid, ectopic lesions, and macrophages of patients suffering from endometriosis in comparison to those without the condition (Pirdel & Pirdel, 2014; Nanda *et al*., 2020; Liu *et al*., 2023); additionally, iron-related metabolic proteins are also increased in these patients (Pirdel & Pirdel, 2014; Nanda *et al*., 2020; Liu *et al*., 2023). Ferroptosis is initiated by an excess of intracellular iron (Ng *et al*., 2020) and represents a form of programmed cell death characterized by lipid peroxidation, a decrease in glutathione peroxidase 4 (GPX4) levels and an imbalance in iron metabolism (Duan *et al*., 2024; Lan *et al*., 2025). FPN deficiency can result in various iron-overload disorders (Cruz *et al*., 2020). The upregulation of FPN, by itself, has the capacity to promote the export of iron, subsequently inhibiting the elevation of intracellular iron concentrations following administration of ferric ammonium citrate (Song *et al*., 2010; Li *et al*., 2021). Disruption in iron metabolism causes iron accumulation at the site of injury, leading to oxidative stress and pro-inflammatory responses that facilitate the progression of endometriosis (EMS) (Wyatt *et al*., 2023; Lan *et al*., 2025).

The concentration of ferritin in serum exhibits a positive correlation with the overall iron reserves in the body. In instances of iron accumulation, surplus iron deposits in the liver, spleen, and various other organs in the form of ferritin, resulting in a marked elevation of serum ferritin concentrations (Cary *et al*., 1982). Serum

ferritin serves as a widely utilized indicator for clinically assessing iron overload. Additionally, ferritin phagocytosis facilitates increased iron release, which can contribute to cellular iron overload (Ni *et al*., 2022; Zhang *et al*., 2024). Extensive research has extensively explored the relationship between serum ferritin levels and female diseases (Ćwiertnia *et al*., 2023; Nulianti *et al*., 2025). In addition, various tissues and organs demonstrate distinct biological responses to iron deposition (Xu *et al*., 2023). Increased ferritin concentrations noted in obese females diagnosed with polycystic ovary syndrome (PCOS) were probably linked to insulin resistance and hyperinsulinemia (Luque-Ramírez *et al*., 2007). Previous research has also suggested a correlation between ferroptosis, iron overload, and infertility in females (Fan *et al*., 2024). Furthermore, the study found a positive association between ferritin levels and the likelihood of gestational diabetes occurring between the 15th and 26th weeks of gestation (aOR=2.43, 95% CI=1.12–5.28; aOR=3.95, 95% CI=1.38–11.30) (Rawal *et al*., 2017; Liu *et al*., 2024). Our results showed that women with elevated serum ferritin levels had an increased risk of endometriosis, and the utilization of RCS analysis revealed a nonlinear association between the two variables, consistent with the findings of (Xu *et al*., 2023; Ratajac *et al*., 2025). The underlying mechanism likely involves disruption of iron homeostasis, facilitating the onset and progression of endometriosis.

In our research, we employed nationally representative data that incorporated sample weights to investigate the association between serum ferritin concentrations and the incidence of endometriosis. We conducted regression analyses adjusting for covariates and using large sample sizes. These analyses facilitated subgroup analyses, enhancing understanding of the model's utility and limitations across diverse patient cohorts, thereby establishing its generalizability. Notably, the incorporation of the lasso and Boruta models in variable selection effectively prevented model overfitting. Through the evaluation of four distinct machine learning algorithms, we constructed a predictive model to ascertain the occurrence of endometriosis and subsequently determined that the RF model was the most effective. This model presents a practical method for predicting individuals who may be at risk of developing endometriosis. The utilization of SHAP facilitated model interpretation, aiding in the identification of key predictors of endometriosis, thereby furnishing tailored insights to inform personalized preventive and clinical management strategies.

This study has several limitations. First, the cross-sectional design precludes determination of temporality and causal inference. Serum ferritin may precede endometriosis, may change because of the disease or its treatment, or may reflect inflammation or other unmeasured conditions; therefore, reverse causation and residual confounding cannot be excluded. Second, endometriosis status was based on self-reported physician diagnosis and was not verified through medical records, imaging, operative reports, or histopathology. This may have resulted in outcome misclassification, including the classification of women with undiagnosed endometriosis in the comparison group. Information on diagnostic methods, disease phenotype, stage, anatomical location, symptom severity, treatment and time since diagnosis was unavailable. Third, the data were collected between 1999 and 2006, and contemporary diagnostic practice increasingly incorporates specialized ultrasound and MRI. Changes in diagnostic awareness, access, protocols, and thresholds may limit the generalizability of these findings to currently diagnosed populations. Fourth, complete-case analysis may have introduced selection bias, and unmeasured inflammatory, metabolic, gynecological, or treatment-related factors may have confounded the observed association. Finally, the machine-learning models underwent internal validation only and were not evaluated in an independent external cohort. Accordingly, the findings should be considered hypothesis-generating and require confirmation in prospective studies using clinically adjudicated cases, including surgically and histologically confirmed endometriosis where available.

The NHANES cycles included in this study were conducted between 1999 and 2006, and diagnostic practices for endometriosis have evolved substantially since that period (Assaf *et al*., 2012; Dong *et al*., 2025)). Contemporary diagnostic pathways increasingly incorporate specialized transvaginal ultrasound and magnetic resonance imaging for the identification and characterization of ovarian and deep endometriosis, whereas diagnosis during the study period may have depended more heavily on symptoms and surgical evaluation (Story and Kennedy, 2004; Khan *et al*., 2025). Changes in clinician awareness, access to imaging, imaging protocols, and diagnostic thresholds may have altered both the probability of receiving a diagnosis and the clinical characteristics of identified cases (Liu *et al*., 2024). Consequently, the case ascertainment and disease spectrum represented in the present study may differ from those of contemporary populations, which may limit the generalizability of the findings.

Accordingly, the present findings should be considered hypothesis-generating rather than clinically confirmatory. Prospective studies are required to establish temporality and to replicate the observed associations in cohorts with clinically adjudicated endometriosis, including cases confirmed by operative findings and, where available, histopathology. Future investigations should also include contemporary imaging-defined phenotypes, inflammatory markers, detailed reproductive and treatment histories, and independent external validation of the machine-learning models.

Conclusions: Our research reveals a significant positive association between serum ferritin concentrations and the likelihood of endometriosis in women residing in the United States. We developed a predictive model based on the random forest algorithm, which showed strong predictive capability. Moving forward, our objective is to incorporate additional pertinent clinical variables and encompass a broader demographic for external validation, thereby delving into potential underlying mechanisms to enhance the efficacy of our risk assessment models.

Funding: This research received no specific grant from any funding agency in the public, commercial, or not-for-profit sectors.

Conflict of Interest: The authors declare that they have no conflict of interest.

Data Availability: The data supporting the findings of this study are included in the manuscript. Additional data are available from the corresponding author upon reasonable request.

Ethics Statement: The original NHANES protocols were approved by the National Center for Health Statistics Research Ethics Review Board. As this study was based exclusively on publicly available, de-identified data, additional institutional ethical approval was not required.

Authors Contribution: Sensen Shi contributed to conceptualization, methodology, investigation, data curation, formal analysis, visualization, and drafting of the original manuscript. Zelong Li contributed to investigation, data curation, formal analysis, and validation. Xinyue Wu and Ziyi Xu contributed to supervision, review, and editing of the manuscript. Junfeng Li contributed to conceptualization, methodology, supervision, project administration, validation, and review and editing of the manuscript. All authors read and approved the final manuscript.

Generative AI Statement: A generative AI-assisted tool was used to support English translation, language editing, grammar correction, readability, and editorial clarity during manuscript preparation. The authors reviewed and revised the relevant text and take full responsibility for the final manuscript.

REFERENCES

Assaf BT, Miller AD, 2012. Pleural endometriosis in an aged rhesus macaque (*Macaca mulatta*): a histopathologic and immunohistochemical study. Veterinary Pathology 49:636-41. doi: 10.1177/0300985811406890.

Avery JC, Deslandes A, Freger SM, *et al*., 2024. Noninvasive diagnostic imaging for endometriosis part 1: a systematic review of recent developments in ultrasound, combination imaging, and artificial intelligence. Fertility and Sterility 121:164-188. https://doi.org/10.1016/j.fertnstert.2023.12.008

Brulport A, Bourdon M, Vaiman D, *et al*., 2024. An integrated multi-tissue approach for endometriosis candidate biomarkers: a systematic review. Reproductive Biology and Endocrinology 22:21. https://doi.org/10.1186/s12958-023-01181-8

Cary CJ, Peter GK and Schiffer SP, 1982. A case report and review of endometriosis in nonhuman primates. Laboratory Animal Science 32:426.

Chin SC, 1994. Endometriosis and pyometra in a Taiwan rhesus (*Macaca cyclopis*). Journal of Chinese Society for Veterinary Science 20:58-64.

Cruz ML, Velazquez-Cruz J, Chompre G, *et al*., 2020. Animals with endometriosis experience beneficial effects and localized modulation of cytokine levels when exposed to voluntary wheel running. The FASEB Journal 34:1-1. https://doi.org/10.1096/fasebj.2020.34.s1.04695

Ćwiertnia A, Kozłowski M and Cymbaluk-Płoska A, 2023. The role of iron and cobalt in gynecological diseases. Cells 12:117. https://doi.org/10.3390/cells12010117

De Corte P, Klinghardt M, von Stockum S, *et al*., 2025. Time to diagnose endometriosis: current status, challenges and regional characteristics—a systematic literature review. An International Journal of Obstetrics & Gynaecology 132:118-130. https://doi.org/10.1111/1471-0528.17973

Dong H, Cao Q, Wang S, *et al*., 2025. miR-128 targets GAREM to regulate the ERK/MAPK signaling pathway and alleviate yak endometritis. Pakistan Veterinary Journal 45(4):1572-1587. http://dx.doi.org/10.29261/pakvetj/2025.330

Dore M, Lagace A, 1985. Spontaneous external endometriosis in a gorilla (*Gorilla gorilla*). Canadian Veterinary Journal 26:347-349.

Duan YH, Wang HL, Liu MN, *et al*., 2024. Reflections on the complex mechanisms of endometriosis from the perspective of ferroptosis. Pathology Research and Practice 259:155353. https://doi.org/10.1016/j.prp.2024.155353

Fan P, Wang Y, Zhang J, *et al*., 2024. Research progress of ferroptosis in female infertility. Journal of Ovarian Research 17:183. https://doi.org/10.1186/s13048-024-01508-y

Gete DG, Doust J, Mortlock S, *et al*., 2024. Risk of iron deficiency in women with endometriosis: a population-based prospective cohort study. Women's Health Issues 34:317-324. https://doi.org/10.1016/j.whi.2024.03.004

Girling JE, 2024. Harnessing the inflammatory processes in endometriosis. Nature Reviews Endocrinology 20:69-70. https://doi.org/10.1038/s41574-023-00937-x

Guo J, He Q and Li Y, 2024. Machine learning-based prediction of vitamin D deficiency: NHANES 2001-2018. Frontiers in Endocrinology 15:1327058. https://doi.org/10.3389/fendo.2024.1327058

Guo S, Jiao X, Li M, *et al*., 2025. The relationship between dietary vitamin B1 and stroke: a machine learning analysis of NHANES data. Frontiers in Nutrition 12:1584654. https://doi.org/10.3389/fnut.2025.1584654

Harder C, Velho RV, Brandes I, *et al*., 2024. Assessing the true prevalence of endometriosis: a narrative review of literature data. International Journal of Gynecology & Obstetrics 167:883-900. https://doi.org/10.1002/ijgo.15756

Hassannia B, Vandenabeele P and Vanden Berghe T, 2019. Targeting ferroptosis to iron out cancer. Cancer Cell 35:830-849. https://doi.org/10.1016/j.ccell.2019.04.002

Hayashi S, Nakamura T, Motooka Y, *et al*., 2020. Novel ovarian endometriosis model causes infertility via iron-mediated oxidative stress in mice. Redox Biology 37:101726. https://doi.org/10.1016/j.redox.2020.101726

Hu YL, Zhang YJ, Lv XY, *et al*., 2024. Impact of Omicron variant infection on female fertility and laboratory outcomes: a self-controlled study. American Journal of Reproductive Immunology 92:e70012. https://doi.org/10.1111/aji.70012

Huang L, Qin W, Su T, *et al*., 2025. Iron metabolism study: the characteristics of iron metabolism in patients with ovarian endometriosis complicated with infertility. Journal of Obstetrics and Gynaecology Research 51:e70058. https://doi.org/10.1111/jog.70058

Kang S, Jin S, Mao X, *et al*., 2024. CD4+ T and CD8+ T cells in uterus exhibit both selective dysfunction and residency signatures. Journal of Immunology Research 2024:5582151. https://doi.org/10.1155/2024/5582151

Khan GZ, Hanif N, Kazmi SUEF, *et al*., 2025. The rising impact of endometritis on infertility in cattle and other large ruminants. Indus Journal of Bioscience Research 3(4):108-121. https://doi.org/10.70749/ijbr.v3i4.1170

Kobayashi H, Imanaka S, Yoshimoto C, *et al*., 2024. Role of autophagy and ferroptosis in the development of endometriotic cysts. International Journal of Molecular Medicine 54:78. https://doi.org/10.3892/ijmm.2024.5402

Lan D, Huang S, Li J, *et al*., 2025. Ferroptosis in endometriosis: traditional Chinese medicine interventions and mechanistic insights. The American Journal of Chinese Medicine 53:385-408. https://doi.org/10.1142/S0192415X25500156

Li H, Hu L, Wang L, *et al*., 2022. Iron activates cGAS-STING signaling and promotes hepatic inflammation. Journal of Agricultural and Food Chemistry 70:2211-2220. https://doi.org/10.1021/acs.jafc.1c06681

Li X, Zhao Y, Zhang D, *et al*., 2023. Development of an interpretable machine learning model associated with heavy metals' exposure to identify coronary heart disease among US adults via SHAP: findings of the US NHANES from 2003 to 2018. Chemosphere 311:137039. https://doi.org/10.1016/j.chemosphere.2022.137039

Li Y, Zeng X, Lu D, *et al*., 2021. Erastin induces ferroptosis via ferroportin-mediated iron accumulation in endometriosis. Human Reproduction 36:951-964. https://doi.org/10.1093/humrep/deaa363

Liu MN, Chen L, Xu TM, *et al*., 2022. Potential clinical implications of iron metabolism in ovarian endometriosis. Journal of Trace

Elements in Medicine and Biology 73:127017. https://doi.org/10.1016/j.jtemb.2022.127017

Liu M, Wu K and Wu Y, 2023. The emerging role of ferroptosis in female reproductive disorders. Biomedicine & Pharmacotherapy 166:115415. https://doi.org/10.1016/j.biopha.2023.115415

Liu R, Wang S, Ren X, *et al*., 2024. Molecular mechanism of miR-184 targets ELK1 to regulate LPS-induced inflammation in yak endometrial epithelial cells. Pakistan Veterinary Journal 44(4):1083-1094. http://dx.doi.org/10.29261/pakvetj/2024.296

Luo Y, Li L, Hu Q, *et al*., 2024. Iron overload increases the sensitivity of endometriosis stromal cells to ferroptosis via a PRC2-independent function of EZH2. The International Journal of Biochemistry & Cell Biology 169:106553. https://doi.org/10.1016/j.biocel.2024.106553

Luque-Ramírez M, Álvarez-Blasco F, Botella-Carretero JI, *et al*., 2007. Increased body iron stores of obese women with polycystic ovary syndrome are a consequence of insulin resistance and hyperinsulinism and are not a result of reduced menstrual losses. Diabetes Care 30:2309-2313. https://doi.org/10.2337/dc07-0642

Mishra A, Galvankar M, Vaidya S, *et al*., 2020. Mouse model for endometriosis is characterized by proliferation and inflammation but not epithelial-to-mesenchymal transition and fibrosis. Journal of Bioscience 45:105. https://doi.org/10.1007/s12038-020-00073-y

Nanda A, Thangapandi K, Banerjee P, *et al*., 2020. Cytokines, angiogenesis, and extracellular matrix degradation are augmented by oxidative stress in endometriosis. Annals of Laboratory Medicine 40:390-397. https://doi.org/10.3343/alm.2020.40.5.390

Ng SW, Norwitz SG, Taylor HS, *et al*., 2020. Endometriosis: the role of iron overload and ferroptosis. Reproductive Sciences 27:1383-1390. https://doi.org/10.1007/s43032-020-00164-z

Ngô C, Chéreau C, Nicco C, *et al*., 2009. Reactive oxygen species controls endometriosis progression. The American Journal of Pathology 175:225-234. https://doi.org/10.2353/ajpath.2009.080804

Ni Z, Li Y, Song D, *et al*., 2022. Iron-overloaded follicular fluid increases the risk of endometriosis-related infertility by triggering granulosa cell ferroptosis and oocyte dysmaturity. Cell Death & Disease 13:579. https://doi.org/10.1038/s41419-022-05037-8

Nulianti R, Bayuaji H, Ritonga MA, *et al*., 2025. Correlation of ferritin and glutathione peroxidase 4 (GPX4) level as a marker of ferroptosis process in endometrioma. Scientific Reports 15:4357. https://doi.org/10.1038/s41598-024-85017-4

Paiva BHA, Silva JF, Ocarino NM *et al*., 2015. A rare case of endometrioma in a bitch. Acta Veterinaria Scandanavia 57:31. https://doi.org/10.1186/s13028-015-0123-1

Pirdel L and Pirdel M, 2014. Role of iron overload-induced macrophage apoptosis in the pathogenesis of peritoneal endometriosis. Reproduction 147:R199-R207. https://doi.org/10.1530/REP-13-0552

Ratajac R, Štrbac F, Petrović J, *et al*., 2025. Evaluation of antibacterial potential of *Satureja montana* L., *Ocimum basilicum* L. and *Salvia officinalis* L. essential oils against reproductive tract pathogens in cattle and their toxicity impact on endometrial and kidney cells. Pakistan Veterinary Journal 45(3):1122-1134. http://dx.doi.org/10.29261/pakvetj/2025.266

Rawal S, Hinkle SN, Bao W, *et al*., 2017. A longitudinal study of iron status during pregnancy and the risk of gestational diabetes: findings from a prospective, multiracial cohort. Diabetologia 60:249-257. https://doi.org/10.1007/s00125-016-4149-3

Santana-Codina N, Quiles Del Rey M, Kapner KS, *et al*., 2022. NCOA4-mediated ferritinophagy is a pancreatic cancer dependency via maintenance of iron bioavailability for iron-sulfur cluster proteins. Cancer Discovery 12:2180-2197. https://doi.org/10.1158/2159-8290.CD-22-0043

Shafrir AL, Farland LV, Shah DK, *et al*., 2018. Risk for and consequences of endometriosis: a critical epidemiologic review. Best Practice & Research Clinical Obstetrics & Gynaecology 51:1-15. https://doi.org/10.1016/j.bpobgyn.2018.06.001

Shaukat A, Rajput SA, Hanif S, *et al*., 2025. Morin inhibits Inflammation, Oxidative stress and Ferroptosis in Lipopolysaccharide-induced Endometritis. Pakistan Veterinary Journal 45(2):799-806. http://dx.doi.org/10.29261/pakvetj/2025.171

Shigetomi H, Imanaka S and Kobayashi H, 2022. Effects of iron-related compounds and bilirubin on redox homeostasis in endometriosis and its malignant transformations. Hormone Molecular Biology and Clinical Investigation 43:187-192. https://doi.org/10.1515/hmbci-2021-0065

Song N, Wang J, Jiang H, *et al*., 2010. Ferroportin 1 and hephaestin overexpression attenuate iron-induced oxidative stress in MES23.5 dopaminergic cells. Journal of Cellular Biochemistry 110:1063-1072. https://doi.org/10.1002/jcb.22617

Story L, Kennedy S, 2004. Animal studies in endometriosis: A review, ILAR Journal 45:132-138. https://doi.org/10.1093/ilar.45.2.132

Tan MY, Zhang YJ, Zhu SX, *et al*., 2025. The prognostic significance of stress hyperglycemia ratio in evaluating all-cause and cardiovascular mortality risk among individuals across stages 0-3 of cardiovascular-kidney-metabolic syndrome: evidence from two cohort studies. Cardiovascular Diabetology 24:137. https://doi.org/10.1186/s12933-025-02689-6

Toyokuni S, 2002. Iron and carcinogenesis: from Fenton reaction to target genes. Redox Report 7:189-197. https://doi.org/10.1179/135100002125000596

Wang T, Yang J, Han Y, *et al*., 2024. Unveiling the intricate connection between per- and polyfluoroalkyl substances and prostate hyperplasia. Science of the Total Environment 932:173085. https://doi.org/10.1016/j.scitotenv.2024.173085

Wyatt J, Fernando SM, Powell SG, *et al*., 2023. The role of iron in the pathogenesis of endometriosis: a systematic review. Human Reproduction Open 2023:hoad033. https://doi.org/10.1093/hropen/hoad033

Xu G, Chen L and Li Q, 2023. Association of iron metabolism markers, socioeconomic and lifestyle factors with endometriosis: a cross-sectional study. Journal of Trace Elements in Medicine and Biology 78:127175. https://doi.org/10.1016/j.jtemb.2023.127175

Yao QZ, Liu RL, Zeng YY, *et al*., 2026. Investigating the association between systemic immune-inflammation index and female fertility: a retrospective cohort study. Journal of Ovarian Research 19:47. https://doi.org/10.1186/s13048-025-01961-3

Zhang J, Su T, Fan Y, *et al*., 2024. Spotlight on iron overload and ferroptosis: research progress in female infertility. Life Sciences 340:122370. https://doi.org/10.1016/j.lfs.2023.122370

Zhang M, Xu T, Tong D, *et al*., 2023. Research advances in endometriosis-related signaling pathways: a review. Biomedicine & Pharmacotherapy 164:114909. https://doi.org/10.1016/j.biopha.2023.114909

Zhang Y, Liu X, Deng M, *et al*., 2022. Ferroptosis induced by iron overload promotes fibrosis in ovarian endometriosis and is related to subpopulations of endometrial stromal cells. Frontiers in Pharmacology 13:930614. https://doi.org/10.3389/fphar.2022.930614

Zhang Y, Xiao L, Lyu L, *et al*., 2024a. Construction of a predictive model for bone metastasis from first primary lung adenocarcinoma within 3 cm based on machine learning algorithm: a retrospective study. PeerJ 12:e17098. https://doi.org/10.7717/peerj.17098

Zondervan KT, Becker CM and Missmer SA, 2020. Endometriosis. New England Journal of Medicine 382:1244-1256. https://doi.org/10.1056/NEJMra1810764

Zuo Z, Zhou Z, Liu Q, *et al*., 2025. Joint association of the triglyceride-glucose index and stress hyperglycemia ratio with incidence and mortality risks of new-onset atrial fibrillation during sepsis: a retrospective cohort study. Cardiovascular Diabetology 24:149. https://doi.org/10.1186/s12933-025-02709-5